

## Electronic origin of the intermediate phase of NiTi

G.-L. Zhao, T. C. Leung, and B. N. Harmon

Ames Laboratory—U.S. Department of Energy and Department of Physics,  
Iowa State University, Ames, Iowa 50011

M. Keil and M. Müllner

Institut für Kernphysik, Universität Frankfurt, D-6000 Frankfurt am Main 90, Federal Republic of Germany

W. Weber\*

Institut für Nukleare Festkörperphysik, Kernforschungszentrum Karlsruhe,  
Postfach 3640, D-7500 Karlsruhe 1, Federal Republic of Germany

(Received 15 May 1989)

A nesting feature in the Fermi surface of ordered, equiatomic NiTi is reported, and related to observed “premartensitic” phenomena.

The shape-memory effect exhibited by NiTi alloys is associated with the martensitic transformation which occurs near room temperature. The high-temperature  $\beta$  phase has the CsCl ( $B2$ ) structure, while the low-temperature martensitic phase is thought to be monoclinic.<sup>1</sup> As temperature is lowered, the martensitic transformation in the equiatomic alloy is preceded by a “premartensitic” or “intermediate,”  $R$ , phase.<sup>2</sup> X-ray, electron, and neutron scattering<sup>3</sup> indicate the development of superlattice peaks near  $\mathbf{Q}_0 = (\frac{1}{3}, \frac{1}{3}, 0)2\pi/a$  in the  $R$  phase.<sup>4</sup> Earlier inelastic-neutron-scattering results suggested an anomaly near this wave vector,<sup>5,6</sup> and more recent results<sup>7-9</sup> indicate that a transverse phonon with wave vector  $\mathbf{Q}_0$  in the CsCl structure goes soft continuously as the temperature is lowered. A calculation of the phonon spectrum<sup>10</sup> which included an evaluation of approximate electron-phonon matrix elements [based on the self-consistent augmented-plane-wave (APW) band structure<sup>11</sup>] failed to show any feature near  $\mathbf{Q}_0$  which would explain the sharp phonon anomaly reported.<sup>8,9</sup> Questions have therefore been raised about possible other driving mechanisms for the anomaly.<sup>12</sup>

We present the results of a new self-consistent band-structure calculation which yields a slightly different Fermi surface for the high-temperature  $\beta$  phase of NiTi. We find that the small differences from the previous calculation<sup>11</sup> do in fact lead to a nesting feature of the Fermi surface, and the nesting wave vector occurs very close to the position observed for the superlattice peaks (actually a few percent smaller than  $\mathbf{Q}_0$ ). Evaluation of the electron-phonon matrix elements using the method of Varma and Weber<sup>13</sup> leads to a soft mode in the lowest  $\Sigma_4$  transverse branch and calculated phonon dispersion curves in good agreement with the neutron-scattering experiments. A more detailed account of our calculations and a more in-depth study of NiTi will be presented elsewhere.

We used a self-consistent first-principles tight-binding method<sup>14</sup> to evaluate the band structure. The results look

very similar to those reported by Papaconstantopoulos *et al.*,<sup>11</sup> with only subtle differences; however, one of those differences occurs on the Fermi surface as shown in Fig. 1. Also shown is the Fermi-surface-nesting wave vector between an unoccupied portion of band 7 and an occupied portion of band 8. The nesting extends for  $k_z$  values between  $-0.2\pi/a$  and  $+0.2\pi/a$ . To evaluate the generalized susceptibility,  $\chi(q)$ , we fit the first-principles band structure in two independent ways. We first used a set of 60 symmetrized plane waves and obtained a rms fitting error for bands 7 and 8 of 1.1 mRy. An empirical, nonorthogonal Slater-Koster (or tight-binding) fit was also made with comparable rms errors. The generalized susceptibility was calculated using the tetrahedron method<sup>15</sup> with the energy eigenvalues obtained from either fit giving nearly identical results. The Fourier series was faster, which allowed the efficient evaluation of more  $\mathbf{q}$  vectors. We show in Fig. 2 those results for  $\mathbf{q}$  along the [110] direction. There is a noticeable rise in the susceptibility from point  $\Gamma$  and to point  $M$  and of particular im-

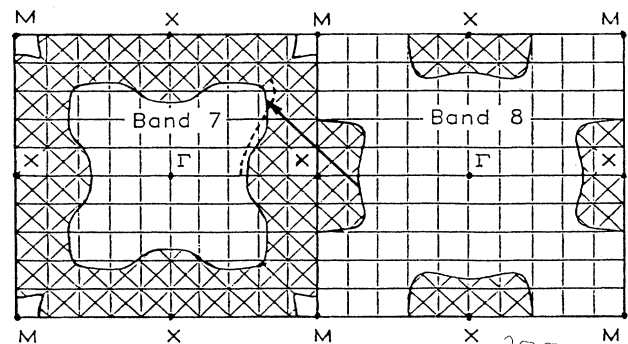


FIG. 1. The Fermi surface for band 7 in the left zone and for band 8 in the right zone. The shaded regions are occupied. The arrow shows the wave vector between the nested regions. The dashed curve is a section of the band-7 Fermi surface reported in Ref. 11.

portance is the small peak which is caused by the nesting feature described above.

A sharp peak in  $\chi(q)$  is frequently associated with charge-density waves (CDW's) and lattice instabilities. Elementary arguments associate CDW's with longitudinal-phonon modes; however, in transition metals the  $d$ -wave functions allow for many types of coupling, and a full evaluation of the electron-phonon matrix elements is required. For example, a similar small peak in the  $\chi(q)$  in fcc La causes a sharp phonon anomaly at  $q=(0.42, 0.42, 0.42)\pi/a$  only in the transverse branch.<sup>16</sup>

To evaluate the electron-phonon matrix elements we have adopted the method of Varma and Weber.<sup>13</sup> We use the full formalism<sup>17</sup> and not the simplified approximation used by Bruinsma.<sup>10</sup> The basic idea is to evaluate accurately the electron-phonon coupling for bands 7 and 8 which cross the Fermi level and give rise to rapidly changing  $q$ -dependent contributions to the dynamical matrix. For the calculation, the Brillouin zone was partitioned into cubes on a  $\pi/20a$  mesh and the electron-phonon matrix elements were assumed constant within each cube. This restricts the evaluation of the dynamical matrix to  $q$  vectors on the same mesh [unlike the  $\chi(q)$  results of Fig. 2]. A few short-range force constants are used as parameters to model the short-range or gradual  $q$ -dependent contributions. The values of the six short-range force constants (1NN Ti-Ni, Ni-Ni, Ti-Ti) were determined by fitting the total theoretical values (obtained from the short-range force constants plus the electronic contribution) to the phonons measured to 400 K.<sup>9</sup> Also, information from phonon density-of-states measurements<sup>9</sup> has been included in the fitting procedure. Phonon frequencies have been measured only for the three acoustic phonon branches along various high-symmetry directions and for a few optic modes very close to the Brillouin-zone center.<sup>5-9</sup> Because of the large incoherent scattering of Ni and the negative coherent scattering amplitude of Ti, the measurement of the optic modes is difficult.

The calculated phonon dispersion curves are in good agreement with the neutron data of the acoustic modes (see Fig. 3). However, the theoretical results predict a

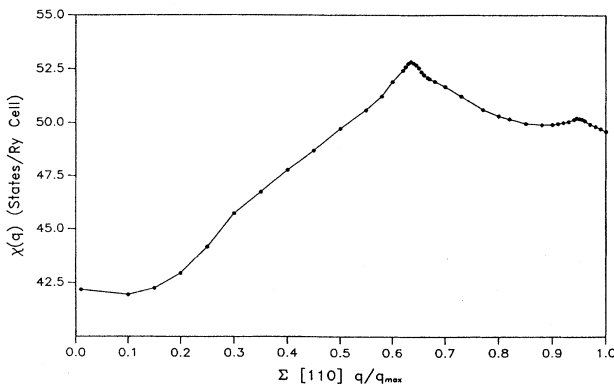


FIG. 2. The generalized susceptibility for NiTi along the [110] or  $\Sigma$  direction. Only bands 7 and 8 which cross the Fermi level were included.

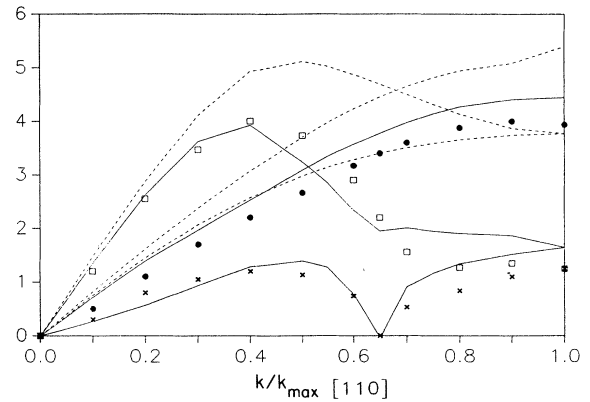


FIG. 3. The phonon dispersion curves along the [110] direction. The data points are from Ref. 9. The dashed lines are the calculated results using only the short-range force constants, while the solid lines are the calculated results including the electron-phonon matrix elements for bands 7 and 8. The frequencies were calculated on a  $k$  mesh of 0.05.

gap between optic and acoustic modes which is not observed in the phonon density-of-states data. It should be noted that any Born-von Kármán model constructed for the interpolation of the experimental phonon data also yields a gap or pseudogap between optic and acoustic modes. We suspect that this discrepancy arises from significant antisite disorder between the Ti and Ni sublattices.

The lack of data for the upper three branches is a problem in arriving at a final theoretical set of short-range parameters. We plan frozen-phonon calculations to provide a totally first-principles phonon spectrum for the completely ordered compound.

Figure 3 exhibits the acoustic branches along the [110] direction. A very strong renormalization of the transverse  $\Sigma_4(110)$  modes due to electron-phonon interaction is observed over the whole range of the  $\Sigma_4$  branch. Also the longitudinal  $\Sigma_1(110)$  branch is drastically lowered towards the zone boundary, where it becomes degenerate with the  $\Sigma_4$  branch. In addition, a strong dip in the  $\Sigma_4$  branch near  $Q=(\frac{1}{3}, \frac{1}{3}, 0)2\pi/a$  is obtained. In fact, the theoretical results, which are  $T=0$  K calculations, indicate a lattice instability. Any finite-temperature effects would smear the nesting and bring theory and experiment into better agreement. This idea is supported by the large measured temperature dependence of the dip.<sup>8</sup>

The coupling of the electrons to the  $\Sigma_4$  branch arises from the geometry of the  $d$  orbitals involved. For  $k$  on the nesting portion of the band-8 Fermi surface the largest component of the wave functions is from the Ni  $d_{x^2-y^2}$  orbital, and for  $k+Q_0$  on the nesting portion of the band-7 Fermi surface the largest component of the wave function is from the Ti  $d_{xy}$  orbital. The matrix elements involving these orbitals are an example of a so-called dormant interaction<sup>17</sup> which results in a particularly large electron-phonon coupling for the  $\Sigma_4$  displace-

ments and little coupling for the longitudinal and [001] transverse displacements.

Besides the extreme temperature dependence of the  $\Sigma_4$  branch near  $(\frac{1}{3}, \frac{1}{3}, 0)2\pi/a$ , the entire  $\Sigma_4$  branch is temperature dependent, with the frequencies becoming smaller as the temperature is lowered. This anomalous temperature dependence is characteristic of the lower transverse [110] branch in many bcc elements. We expect the anharmonic couplings responsible for this behavior to be similar to those we have previously studied for the bcc-to-hcp transition in Zr.<sup>18</sup> The anharmonic interactions in the entire  $\Sigma_4$  branch are responsible for driving the martensitic transformation. The transformation to the intermediate phase, on the other hand, is caused by the nesting and resulting dip in the  $\Sigma_4$  branch, with an added contribution from the general lowering of the  $\Sigma_4$  branch (with decreasing temperature) which helps to push the  $Q_0$

phonon to lower frequencies and eventually soft. Thus, the "premartensitic" phase in NiTi is present only because of a subtle feature of its Fermi surface, and exactly similar premartensitic phenomena are not in general expected to accompany martensitic transformations in other alloys.

One of us (B.N.H.) is grateful to L. Tanner and S. Shapiro for useful discussions. Ames Laboratory is operated for the U.S. Department of Energy by Iowa State University under Contract No. W-7405-Eng-82. This work was supported by the Director for Energy Research, Office of Basic Energy Sciences of the U.S. Department of Energy. This work was also supported by the Bundesminister für Forschung und Technologie (Bonn, Germany).

\*Present address: Institut für Theoretische Physik II, Universität Dortmund, D-4600 Dortmund, Federal Republic of Germany.

<sup>1</sup>W. Bühner, R. Gotthardt, A. Kulik, O. Mercier, and F. Staub, *J. Phys. F* **13**, L77 (1983).

<sup>2</sup>A large literature exists, and many earlier references may be found in V. G. Pushin, V. V. Kondrat'ev, and V. N. Khachin, *Izv. Vyssh. Uchebn. Zaved. Fiz.* **5**, 5 (1985) [*Sov. Phys. J.* **28**, 341 (1985)]; also, H. C. Ling and R. Kaplow, *Mater. Sci. Eng.* **51**, 193 (1981).

<sup>3</sup>Further references may be found in S. M. Shapiro, Y. Noda, Y. Fujii, and Y. Yamada, *Phys. Rev. B* **30**, 4314 (1984).

<sup>4</sup>Superlattice peaks are also observed at the " $\omega$ -phase" wave vector  $(\frac{1}{3}, \frac{1}{3}, \frac{1}{3})2\pi/a$ ; however, these may be related to multiple- $Q_0$  configurations and need not involve a softening of the  $\omega$ -phase phonon. See Ref. 3, and also I. Folkins and M. B. Walker, *Phys. Rev. B* **40**, 255 (1989).

<sup>5</sup>W. Bühner, O. Mercier, P. Brüesch, and R. Gotthardt, Eidgenössische Technische Hochschule Zürich Report No. AF-SSP-115, p. 60 (1981).

<sup>6</sup>S. K. Satija, S. M. Shapiro, M. B. Salamon, and C. M. Wayman, *Phys. Rev.* **29**, 6031 (1984).

<sup>7</sup>P. Moine, J. Allain, and B. Renker, *J. Phys. F* **14**, 2517 (1984).

<sup>8</sup>H. Teitze, M. Müllner, and B. Renker, *J. Phys. C* **17**, L529 (1984).

<sup>9</sup>M. Müllner, G. G. Herget, M. Keil, G. Eckold, J. B. Suck, W. Weber, and H. Jex (unpublished).

<sup>10</sup>R. Bruinsma, *Phys. Rev. B* **25**, 2951 (1982).

<sup>11</sup>D. A. Papaconstantopoulos, G. N. Kamm, and P. N. Pouloupoulos, *Solid State Commun.* **41**, 93 (1982); J. Shore and D. Papaconstantopoulos, *J. Phys. Chem. Solids* **45**, 437 (1984).

<sup>12</sup>J. A. Krumhansl, in *Nonlinearity on Condensed Matter*, edited by A. R. Bishop, D. K. Campbell, P. Kumar, and S. E. Trullinger (Springer-Verlag, Berlin, 1986), p. 255.

<sup>13</sup>C. M. Varma and W. Weber, *Phys. Rev. Lett.* **39**, 1094 (1977); *Phys. Rev. B* **19**, 6142 (1979).

<sup>14</sup>J. A. Appelbaum and D. R. Hamann, in *Transition Metals, IOP Conf. Proc. No. 39*, edited by M. J. G. Lee, J. M. Perz, and E. Fawcett (Institute of Physics, Bristol, 1977), p. 111; P. J. Feibelmann, J. A. Appelbaum, and D. R. Hamann, *Phys. Rev. B* **20**, 1433 (1979); B. N. Harmon, W. Weber, and D. R. Hamann, *ibid.* **25**, 1109 (1982).

<sup>15</sup>J. Rath and A. J. Freeman, *Phys. Rev. B* **11**, 2109 (1975).

<sup>16</sup>X. W. Wang, B. N. Harmon, Y. Chen, K. M. Ho, C. Stassis, and W. Weber, *Phys. Rev. B* **33**, 3851 (1986).

<sup>17</sup>W. Weber, in *Physics of Transition Metals, 1980*, IOP Conf. Proc. No. 55, edited by P. Rhodes (Institute of Physics, Bristol, 1980).

<sup>18</sup>Y. Y. Ye, Y. Chen, K. M. Ho, B. N. Harmon, and P. A. Lindgård, *Phys. Rev. Lett.* **58**, 1769 (1987).